

Supporting Information

Photo-gain optimization in multilayer organic phototransistors by study of space-charge limited current

Giulia Baroni¹, Francesco Reginato¹, Mario Prosa¹, Marco Brucale¹, Federico Prescimone¹, Mirko Seri, Katherine Gallegos-Rosas², Caterina Soldano², Margherita Bolognesi¹, *, Stefano Toffanin¹, *

¹ Consiglio Nazionale delle Ricerche (CNR) Istituto per lo Studio dei Materiali Nanostrutturati (ISMN), 40129 Bologna (Italy)

² Department of Electronics and Nanoengineering, Aalto University, 00250 Espoo (Finland)

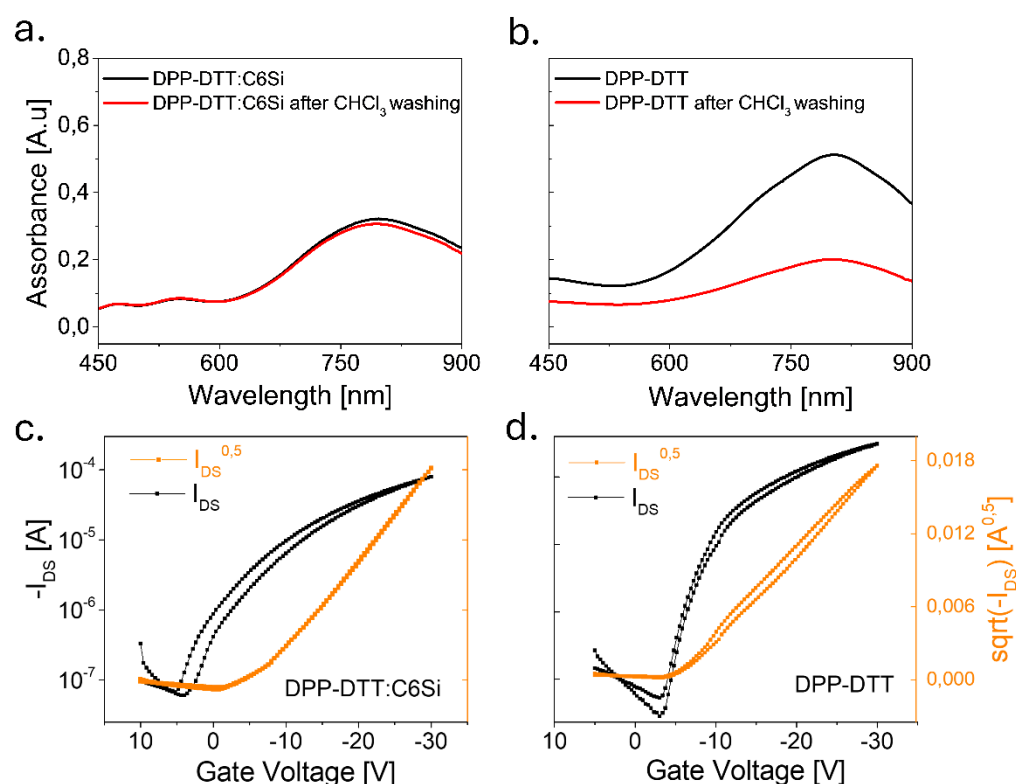


Figure S1. Cross-linked DPP-DTT:C6Si characterization: (a-b) The absorption spectra of the two different HTL after CHCl₃ washing (c-d) Transfer characteristics of transistors with different HTL ($V_{DS} = -30$ V), including, (c) cross-linked DPP-DTT:C6Si film, (d) pristine DPP-DTT film.

	μ_p^{FET} [cm ² /(V s)]	V _{th} [V]	I _d /I _g @V _g =-30V	I _{on} /I _{off}
DPP-DTT	10 ⁻¹	-4	10 ³	10 ³
DPP-DTT:C6Si	10 ⁻²	-7	10 ³	10 ³

Table S1: Performance parameters of the OFETs fabricated with pristine DPP-DTT and DPP-DTT crosslinked by C6Si. Each value has been extrapolated from transfer curve measured in dark conditions.

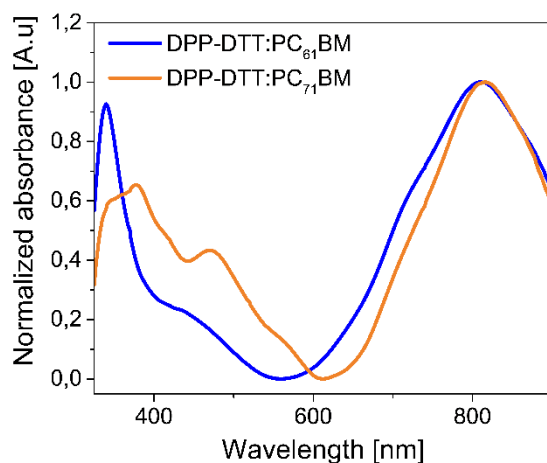


Figure S2. Normalized absorption spectra of the BHJs.

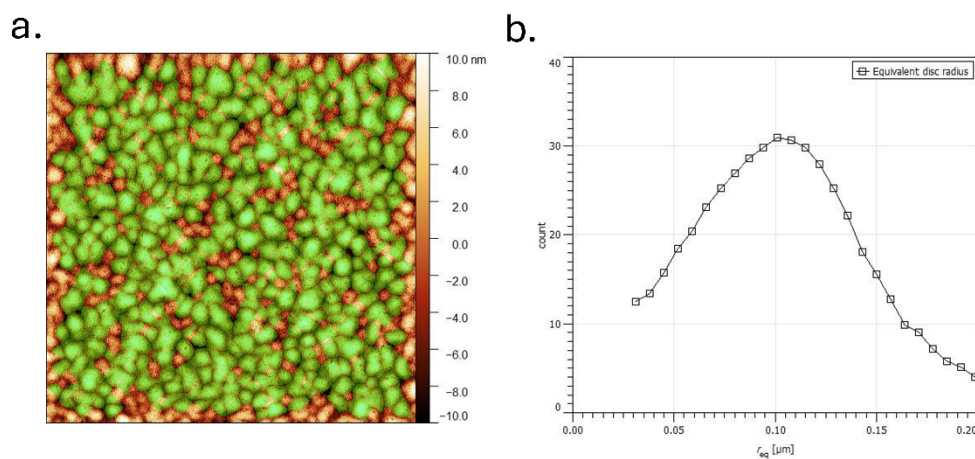


Figure S3. (Left): Example of granular domain measurement from AFM micrographs for a DPP-DTT:PC71BM-CHCl₃ film. Lateral size is 5x5μm Individual domains were automatically outlined via the Gwyddion segmentation algorithm after a 7px Gaussian Smoothing. (Right): Equivalent disc radius from

several individual grains is plotted as equivalent disc radius values. The resulting size distribution is monomodal with a mode of $\sim 100\text{nm}$, corresponding to a mean grain diameter of $\sim 200\text{nm}$.

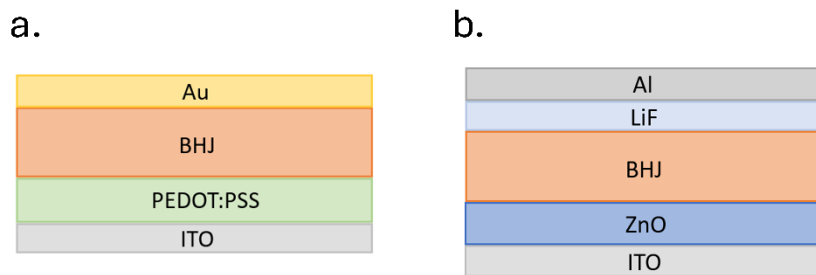


Figure S4: Schematic device structure of (a) HOD and (b) EOD device structures.

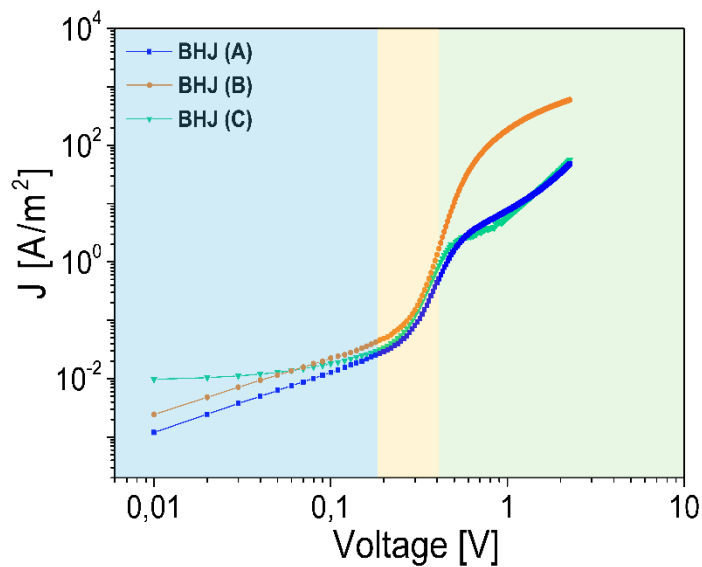


Figure S5: J-V curves of the hole-only devices with structure ITO/PEDOT:PSS/BHJ/Au in which the three typical charge-transport regions are clearly visible: (i) ohmic region ($J \propto V$) highlighted in blue, (ii) trap-SCLC region ($J \propto V^n$) region in yellow and (iii) SCLC region ($J \propto V^2$) in green.

BHJ	Annealing	$\mu^{\text{SCLC}}_{\text{p}}$ [cm ² /Vs] @10V	$\mu^{\text{SCLC}}_{\text{n}}$ [cm ² /Vs] @10V
(C)	135°C for 10'	$3,4 \cdot 10^{-5}$	$1,1 \cdot 10^{-6}$
(C)	-	$1,2 \cdot 10^{-5}$	$7,3 \cdot 10^{-5}$

Table S2 Performance parameters of the HODs and EODs fabricated with the BHJ based on DPP-DTT:PC₆₁BM processed from the CHCl₃:ODCB solvent mixtures, with and without annealing post-process on the BHJ. Each value has been extrapolated from measurements on 2 different devices.

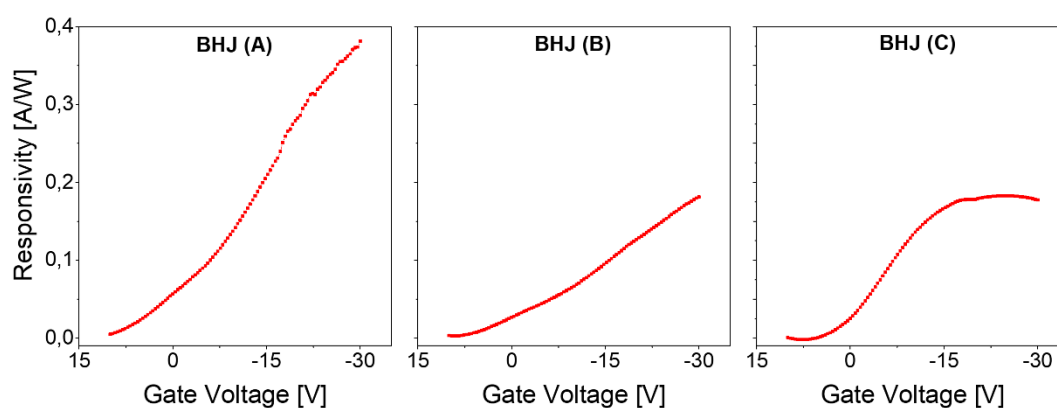


Figure S6. Light responsivity R as function of the applied gate voltage V_g of multilayer OPTs with BHJ photoactive layer (a) **(A)**, (b) **(B)** and (c) **(C)**.

The data supporting this article have been included as part of the Supplementary Information.

Multiple Output Curve of OPT fabricated with the BHJ based on DPP-DTT:PC₆₁BM processed from the CHCl₃



PC60-CF-moc p
vd-20.csv

Multiple Output Curve of OPT fabricated with the BHJ based on DPP-DTT:PC₇₁BM processed from the CHCl₃



PC70-CF-moc p
vd-20.csv